

Model Predictive Control of a Shared Autonomous Electric Vehicles system with charge scheduling and electricity price response

Riccardo Iacobucci

Graduate School of Energy Science
Kyoto University

Yoshida Honmachi, Kyoto, Japan

Email: iacobucci.riccardo.38e@kyoto-u.jp

Benjamin McLellan

Graduate School of Energy Science
Kyoto University

Yoshida Honmachi, Kyoto, Japan

Email: b-mclellan@energy.kyoto-u.ac.jp

Tetsuo Tezuka

Graduate School of Energy Science
Kyoto University

Yoshida Honmachi, Kyoto, Japan

Email: tezuka@energy.kyoto-u.ac.jp

Abstract—Shared autonomous electric vehicles (SAEVs), also known as autonomous mobility on demand systems, are expected to soon be commercially available. This work proposes a methodology for the optimization of SAEV charging taking into account optimized vehicles routing and rebalancing. The methodology presented is based on previous work expanded to include charge scheduling optimization. Our model deals with the different time frames at which transport service and charging have to be optimized with a model-predictive control optimization routine which is run in parallel at two different time scales. Vehicle charging is optimized over longer time scales to minimize waiting times for passengers and electricity costs. Routing and rebalancing is optimized at shorter time-scales to minimize waiting times for passengers, taking as charging constraints the results of the long-time-scale optimization. This approach allows the efficient optimization of both aspects of SAEV operation. The problem is solved as a mixed-integer linear program. A case study using real transport data for Tokyo is used to test the model, showing that the system can substantially cut charging costs while keeping passenger wait times low.

Index Terms—shared transportation, autonomous vehicles, electric vehicles, demand response, charge scheduling

I. INTRODUCTION

Internet and smartphones are opening the way for new shared models of transportation. One-way car sharing services, in which cars can be taken at wherever they are currently parked and left at any other place within an area, are already popular in large cities in Europe [1]. Autonomous driving technology could speed up the adoption of this transport mode, making it more convenient [2].

This change of paradigm has important implications from the point of view of energy use, since it could allow a faster electrification of the transport sector and enable a more efficient control of the charging of vehicles [3]. It is therefore important to study the impact of this system on the electricity grid. However, studies on shared autonomous vehicles have mainly only dealt with the transport aspects, without considering charging optimization. Most of the literature on the charging of electric vehicles have focused on private vehicles, mostly assuming that vehicles are used once or twice a day and charged at home at night [4], [5], [6].

In this work, a charge optimization based on electricity price is integrated into a model predictive control (MPC) of a shared autonomous electric vehicle (SAEV) system based on the work by Zhang et al. [7]. The novel model deals with the different time frames at which transport service and charging have to be optimized with a MPC optimization which is run in parallel at two different time scales. Vehicle charging is optimized over longer time scales to minimize electricity costs. Vehicle routing and rebalancing for transport service is optimized at shorter time-scales to minimize waiting times for passengers, taking as constraints the results of the long-time-scale optimization. This approach allows the efficient optimization of both aspects of SAEV operation.

II. METHODOLOGY

This work is based on the work by Zhang et al. [7] where an MPC was developed to find optimal management strategies for rebalancing of autonomous mobility-on-demand systems (shared autonomous vehicles). The work also proposed a version with charging constraints. However, the charging was not optimized and the vehicles were assumed to charge at maximum power as soon as they connect to charging stations.

A. Transport model from literature

The problem is formulated as a mixed integer linear program (MILP). The problem formulation ensures that the system always optimize the rebalancing of the vehicles within the optimization horizon, however the computational complexity of the solution is such that the optimization is feasible only for relatively small systems (in the order of few tens of nodes). This is an important limit in the practical implementation of this MPC, but nevertheless its results can be useful to estimate the performance of other systems in comparison.

In this work, the model is extended to include electricity price-based charge scheduling to the global optimization.

The model evolves according to:

$$x(t+1) = Ax(t) + Bu(t) + c(t) \quad (1)$$

where $x(t)$ is the state of the system, $u(t)$ is the set of control variables and $c(t)$ represents new passenger arrivals at nodes. These variables are composed of rearranged variables described as follows. The controls for the optimization are encoded into binary variables. $v_{ij}^k(t) = 1$ when vehicle k is transporting passengers between i and j and $w_{ij}^k(t)$ is similarly defined for rebalancing trips (empty trips). $d_{ij}(t)$ and $c_{ij}(t)$ are, respectively, the number of passengers waiting and arriving at node i with destination j at time t . $d_{ij}(t)$ evolves as:

$$d_{ij}(t+1) = d_{ij}(t) + c_{ij}(t) - \sum_k v_{ij}^k(t) \quad (2)$$

Another variable is used to keep track of vehicles in movement: $T_i p_i^k(t) = 1$ when vehicle k is at distance T_i from its destination i at time t . This evolves as:

$$T_i p_i^k(t+1) = \begin{cases} T_i^{+1} p_i^k(t) + \sum_{j: t_{ji}-1=T_i} (v_{ij}^k(t) + w_{ij}^k(t)) & T_i < T_{max,i} \\ \sum_{j: t_{ji}-1=T_i} (v_{ij}^k(t) + w_{ij}^k(t)) & T_i = T_{max,i} \end{cases} \quad (3)$$

The binary variable $u_i^k(t)$ is used to record waiting vehicles at nodes. $u_i^k(t) = 1$ when vehicle k is waiting at node i at time t . The variable evolves as:

$$u_i^k(t+1) = u_i^k(t) + 0 p_i^k(t) - \sum_k (v_{ij}^k(t) + w_{ij}^k(t)) \quad (4)$$

Vehicles can either be waiting or be moving:

$$\sum_i u_i^k(t) + \sum_{i, T_i} T_i p_i^k(t) \quad (5)$$

Also, vehicles can only do one action at each time step:

$$\sum_i \left(u_i^k(t) + \sum_j v_{ij}^k(t) + \sum_j w_{ij}^k(t) \right) \leq 1 \quad (6)$$

and vehicles cannot transport more passengers than there are waiting at stations:

$$\sum_k v_{ij}^k(t) \leq d_{ij}(t) + c_{ij}(t) \quad (7)$$

Another constraint is associated with vehicles' charge state. The state of charge (SOC) of vehicles is encoded into a real variable $q^k(t)$ with $0 \leq q_{min} \leq q^k(t) \leq q_{max} \leq 1$. Vehicles need to have enough charge to be assigned a trip:

$$q^k(t) \geq v_{ij}^k(t) \alpha_d t_{ij} + q_{min} \quad (8)$$

$$q^k(t) \geq w_{ij}^k(t) \alpha_d t_{ij} + q_{min} \quad (9)$$

α_d is the energy consumption per time step, and t_{ij} is the number of time steps for the trip from i to j .

The cost functions to minimize are related to the waiting time for passengers and the rebalancing costs:

$$J_x(x(t)) = \sum_{i,j} d_{ij}(t) \quad (10)$$

$$J_u(u(t)) = \sum_k \sum_{i,j} t_{ij} w_{ij}^k(t) \quad (11)$$

For a more detailed explanation of the model, refer to [7]. In the original work, the charging was not controlled by the optimization, but was an automatic feature of vehicles idle in a node. When a vehicle was not moving, the vehicle is assumed to be charging at a fixed charging rate until full state of charge or a movement is requested.

B. Charge scheduling

In this work the charging was added to the control vector, thus becoming part of the optimization. The state of charge $q^k(t)$ therefore evolves as:

$$q^k(t+1) = q^k(t) + e^k(t) \quad (12)$$

where $e^k(t)$ is the energy charged in time step t .

The constraints for the charging rates are:

$$0 \leq e^k(t) \leq \alpha_c \sum_i u_i^k \quad (13)$$

where α_c is the maximum charging rate.

To take into account the charging rate in the optimization, a further cost function is added. This is stated as:

$$J_m(u(t)) = \sum_{k \in V} e^k(t) m(t) \quad (14)$$

where $m(t)$ is the price of electricity, which is considered not affected by the system (price taker). Cost function J_m is added as a further objective to the cost functions relative to the waiting time for passengers J_x and the redistribution trips for vehicles J_u .

Another cost function is added to put a premium on higher state of charge at the end of the optimization period:

$$J_s = - \sum_{k \in V} q^k(t + t_{hor} - 1) \quad (15)$$

with t_{hor} the optimization horizon. The overall objective is therefore (the variables for each function have been omitted for compactness and clarity):

$$\underset{u(t), \dots, u(t+t_{hor}-1)}{\text{minimize}} \sum_t \left(J_x + \rho_1 J_u + \rho_2 J_m \right) + \rho_3 J_s \quad (16)$$

ρ_1 , ρ_2 , and ρ_3 in (16) are the relative weights assigned to each secondary objective.

C. Model predictive control

In model predictive control (or receding horizon control), at each time step the optimization is performed over a time horizon and only the first control action is executed. This ensures that at each time step the control takes into account all the information available up to the future prediction horizon when taking the present action.

D. Two-layer optimization

The time scales of transport planning and energy storage planning are very different. While transport rebalancing is generally optimized with an horizon of 15 minutes to half an hour [7], [8], electric vehicles charging is generally optimized over at least several hours. This is due to several considerations. First of all, charging is relatively slow, and even in the case of fast-charging it may take over an hour to fully charge an electric vehicle battery. Moreover, it is more efficient to be able to charge for a relatively long time once a vehicle is connected, since continuous connection and disconnection may waste time.

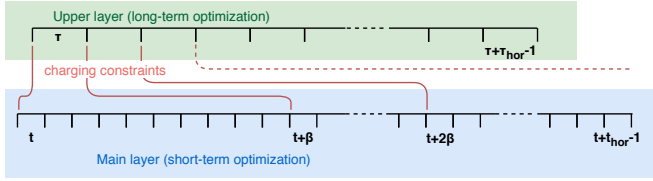


Fig. 1: Schematic diagram of the two-layers MPC optimization model

The most important consideration however is related to the opportunities that these vehicles offer to the grid. In order to provide a service to the grid and avoid grid congestion, the charge scheduling algorithm needs to be able to optimize over the time frame of variability of electricity demand and intermittent renewable energy sources such as wind and solar, which can be several hours.

In order to optimize both transport and charging, a two-layers optimization was developed. A higher ‘coarse’ MPC layer optimizes for charging over longer time frames taking into consideration the approximate necessities of transport service. The main layer optimizes transport service over short time frames, taking as constraints the optimal charging schedule found by the higher layer. Both layers are based on the model presented in the previous sections. However, charging schedule in the main lower layer becomes a constraint, determined by the long-term coarse optimization layer.

The two layers are related by a step length ratio β that determines the relative length of a time step between the two layers. At the beginning of the simulation, the higher coarse layer determines the optimal charging schedule by optimizing over its own time frame. The results are passed down to the main layer as constraints on charging during each step. After β time steps in the main layer, the higher layer optimizes again over its own time frame, passing down the next charging constraints to the main layer for the next β time steps.

E. Constraint assignment

In this section, the upper layer simulation variables are denoted with Greek letters, so that d , p , u , q , t , e are respectively δ , π , μ , ϕ , τ , ϵ . We also define T_i^k as the distance from node i of vehicle k if moving, and $T_i^k = 0$ if the vehicle is waiting at node i . At the start of a upper layer simulation at

(main) time t' , we assign the main layer situation to the upper layer:

$$\delta_{ij}(\tau) = d_{ij}(t') \quad (17)$$

$$\lceil T_i^k / \beta \rceil \pi_i^k(\tau) = 1 \quad \text{if } T_i^k > 0 \quad (18)$$

$$\mu_i^k(\tau) = u_i^k(t') \quad (19)$$

$$\phi^k(\tau) = q^k(t') \quad (20)$$

The charging controls resulting from the upper layer optimization are assigned back to the main layer as constraints on charging and on movement. For vehicles moving, the constraints are valid only after the arrival.

$$e^k(t) = \begin{cases} \epsilon^k(\tau') / \beta & t > t' + T_i^k \\ 0 & t \leq t' + T_i^k \end{cases} \quad (21)$$

$$u_i^k(t) = \begin{cases} 1 & t > t' + T_i^k \\ 0 & t \leq t' + T_i^k \end{cases} \quad (22)$$

where τ' in (21) such that $(\tau - 1)\beta < t' - t \leq \tau\beta$.

III. RESULTS

The problem was solved as a mixed integer linear optimization with the built-in MATLAB function *intlinprog*. To evaluate the performance of the model, several simulations were conducted using data from a transport survey in Tokyo.

A. Transport survey data

The Tokyo Person Trip Survey 2008 [9] is a survey of around 2 million trips in the Tokyo metropolitan area. The 2008 survey is the latest available survey released for Tokyo. Although somewhat old, the demographics and infrastructure of Tokyo has remained stable and it is expected that this implies a relatively stable demand pattern when compared to 2008. The survey associates the origins and destinations of trips to zones, corresponding to specific addresses in Tokyo. These geographical zones were used in the model as the reference nodes. The geographic coordinates of the zones were found from the addresses reported in the survey using the Google Maps Geocoding API [10]. A central 10x10km area of Tokyo was chosen for the simulations, approximately equivalent to the 6 most central special wards of the city. This area was divided into 10 regions by grouping nodes with k-means clustering. The cluster’s centroid for each area was considered as a discretized model of the origin/destination of trips in each area (Fig. 2). For this study, only trips by car or taxi were considered, representing about 20% of the total trips in the survey. These are the trips with characteristics more likely to be similar to trips done with the SAEV system. Each trip in the survey also has a starting time and a weight. The weight is used to indicate the relative significance of that specific trip and to normalize the survey results over the total demographics of Tokyo. Each selected trip k is then defined with four values $[rw_k, rt_k, ro_k, rd_k]$ to indicate respectively associated weight, hour of departure (0-23), origin node, and

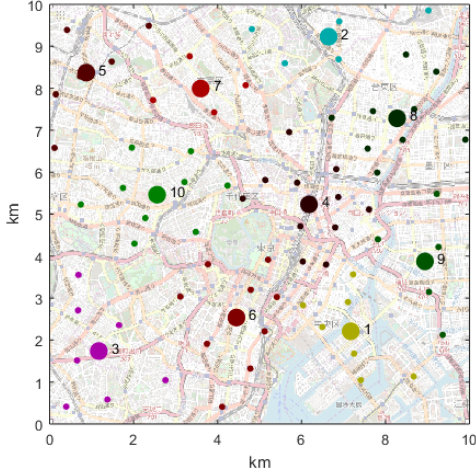


Fig. 2: Map of nodes and clusters with centroids in central Tokyo. From [9].

destination node. The probability $p_{i,j}(t)$ of a trip from i to j at time step t was found as:

$$p_{i,j}(t) = \frac{\sum_{k'} r w_{k'}}{\sum_k r w_k}, \quad (23)$$

$$k : rt_k = t', k' : rt_{k'} = t', ro_{k'} = i, rd_{k'} = j$$

where $t' = \lfloor ((t \cdot \ell - 1) \bmod 1440) / 60 \rfloor$ is the hour of the day corresponding to time step t , with ℓ the length of the time step in minutes. The relative number of trips departing at hour h from the survey is:

$$f(h) = \frac{\sum_{k'} r w_{k'}}{\sum_k r w_k}, \quad k' : rt_{k'} = h \quad (24)$$

At each time step t (at hour of the day h), the rate of arrivals is then:

$$\lambda(t) = TPD \cdot f(t') \cdot \ell / 60 \quad (25)$$

where TPD is the rate of trips per day. A Poisson process with the rate in (25) was used to generate the number of stochastic arrivals at each time step, with origin and destination nodes selected according to (23).

B. Charge scheduling performance

Simulations were run with a random electricity price profile sampled from a gamma distribution with shape parameter 2 and scale parameter 10, giving an average electricity price of 20 JPY. The random profile was chosen to simulate a grid with very high penetration of non-dispatchable renewable energy, as the current electricity market in Japan has low penetration of intermittent renewable energy and its profile has low variability. The price is assumed to change in 20 minutes intervals (72 different prices in a day). The speed of vehicles was chosen at 20 km/h, the reported average road speed in central Tokyo at peak time [11]. The system studied was composed of the 10 nodes identified by the cluster's centroids, 20 vehicles, and an average trip rate of

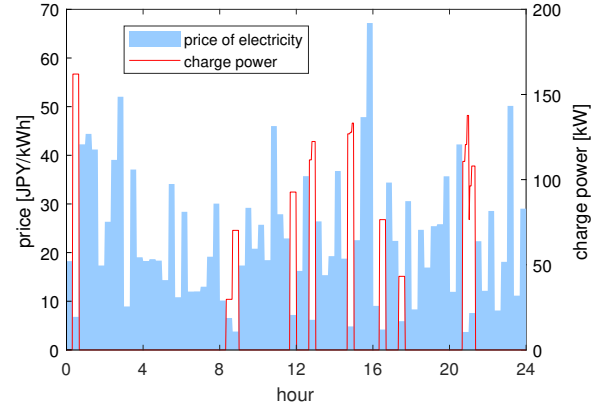


Fig. 3: Aggregated charging power and electricity price for the 2-layer model

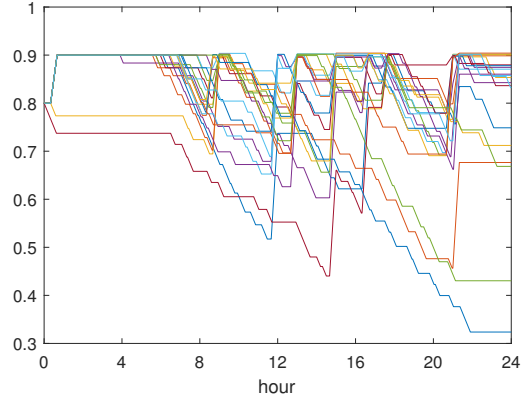


Fig. 4: State of charge (SOC) of vehicles for the 2-layer model

300 trips per day. The main layer has a 2 minute time step, and 20 time steps horizon (40 minutes). The time step length was chosen as a compromise between time resolution and acceptable computational times. The long time horizon is necessary because of the large area served by the vehicles and the time it takes to rebalance, as traveling between the two farthest nodes takes about 45 minutes. The ratio between the two layers is chosen as $\beta = 10$, so that the higher layer has a time step of 20 minutes. The time horizon for the higher layer is set at 8, giving an optimization time frame of 2 hours and 40 minutes. This was chosen as a compromise between better optimization and computational time. Longer horizons may be suitable for electricity price profiles with slower changes or longer periodicity, however requiring longer computational times. Vehicles battery size was chosen at 30 kWh and the state of charge was limited between 0.2 and 0.9.

We compare our proposed model with the unscheduled charging model presented in [7], where vehicles charge at maximum power as soon as they are idle. The unscheduled model was created by only running the main optimization, with the objective function in (14) modified to:

	unscheduled	1-layer	2-layers
mean wait time (seconds)	38	30	22
peak wait time (minutes)	6	13	10
total electricity cost (yen)	10,718	5,679	1,790

TABLE I: Summary of results for the 3 models

$$J_m(u(t)) = \sum_{k \in V} e^k(t) \quad (26)$$

and setting $\rho_2 = 10^{-6}$ and $\rho_3 = 0$. The very low secondary objective weight effectively ensures that vehicles charge whenever they are waiting at nodes while not affecting the transport optimization model. Results presented are for simulation with the same price profile and transport demand.

In Fig. 3, aggregated charging power and electricity price profile during the day is presented for the proposed model. Vehicles tend to charge during periods of lowest electricity prices. It should be noted that in case of short term optimization, vehicles would not ‘see’ the optimal electricity price, tending to charge at sub-optimal local minima. For short time horizons, vehicles would effectively see only one constant price, making optimization impossible. Fig. 4 shows the evolution of the vehicles’ state of charge (SOC) during simulation time.

The 10-minutes moving average waiting times for new arrivals for the two models is shown in Fig. 5. The results of the simulations are summarized in table I. The proposed two-layer scheduled model cut electricity costs by over 80% compared to the unscheduled algorithm, and by almost 70% compared to the 1-layer optimization, while keeping waiting times low. Compared to the unscheduled model, the 10-minutes moving average peak waiting time increases from 6 minutes to 10 minutes, while the average waiting time decreases from 38 seconds to 22 seconds, thanks to the longer optimization horizon. In both cases, including charge optimization increases maximum waiting times as a trade-off between optimal charging and optimal transport service is introduced.

The median computation time for a time step on a quad-core 3 GHz Intel Core i5 processor with 32GB of RAM was 4.2 seconds for the upper layer and 3.1 seconds for the main layer. The average overall was 3.8 seconds per time step.

IV. CONCLUSIONS AND FURTHER WORK

An extension of the model presented in [7] was developed to include vehicle charging optimization with price information from the grid with two-layer parallel optimization at different time scales. The results show that the proposed method can reduce the costs of the system by over 80% without significantly impacting waiting times. While peak wait times increase by 66%, mean wait times decreases thanks to the longer optimization horizon. We think that as the penetration of electrified transportation increases, charge scheduling will play an increasingly important role in avoiding grid congestion. These results show that it is possible to optimize both without negative effect on transport service.

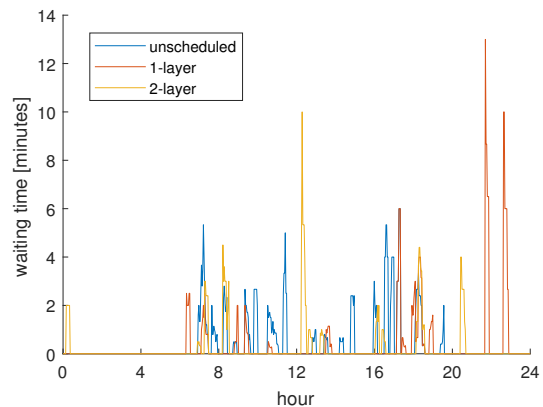


Fig. 5: 10 minutes moving average waiting times

Several further aspects could be investigated in future work. The model could be extended to allow for selection of which nodes are charging stations. Moreover, an extension could include the optimization of energy delivery back to the grid with vehicle-to-grid (V2G) technology. Other ancillary services such as operating reserve could also be provided by the system, and their potential could be investigated by including them in the global optimization.

REFERENCES

- [1] B. Boyacı, K. G. Zografos, and N. Geroliminis, “An optimization framework for the development of efficient one-way car-sharing systems,” *European Journal of Operational Research*, vol. 240, pp. 718–733, Feb. 2015.
- [2] D. J. Fagnant and K. M. Kockelman, “The travel and environmental implications of shared autonomous vehicles, using agent-based model scenarios,” *Transportation Research Part C: Emerging Technologies*, vol. 40, pp. 1–13, Mar. 2014.
- [3] J. Weiss, R. Hledik, R. Lueken, T. Lee, and W. Gorman, “The electrification accelerator: Understanding the implications of autonomous vehicles for electric utilities,” *The Electricity Journal*, vol. 30, pp. 50–57, Dec. 2017.
- [4] J. C. Mukherjee and A. Gupta, “A Review of Charge Scheduling of Electric Vehicles in Smart Grid,” *IEEE Systems Journal*, vol. 9, pp. 1541–1553, Dec. 2015.
- [5] L. Liu, F. Kong, X. Liu, Y. Peng, and Q. Wang, “A review on electric vehicles interacting with renewable energy in smart grid,” *Renewable and Sustainable Energy Reviews*, vol. 51, pp. 648–661, Nov. 2015.
- [6] D. B. Richardson, “Electric vehicles and the electric grid: A review of modeling approaches, impacts, and renewable energy integration,” *Renewable and Sustainable Energy Reviews*, vol. 19, pp. 247–254, Mar. 2013.
- [7] R. Zhang, F. Rossi, and M. Pavone, “Model predictive control of autonomous mobility-on-demand systems,” in *2016 IEEE International Conference on Robotics and Automation (ICRA)*, pp. 1382–1389, May 2016.
- [8] K. Spieser, K. Treleaven, R. Zhang, E. Frazzoli, D. Morton, and M. Pavone, “Toward a Systematic Approach to the Design and Evaluation of Automated Mobility-on-Demand Systems: A Case Study in Singapore,” in *Road Vehicle Automation* (G. Meyer and S. Beiker, eds.), pp. 229–245, Cham: Springer International Publishing, 2014.
- [9] Ministry of Land, Infrastructure, Transport and Tourism, Japan (MLIT), “Tokyo Metropolitan Area Person trip survey,” 2008.
- [10] “Developer’s Guide | Google Maps Geocoding API.”
- [11] Tokyo Metropolitan Government Environment Bureau, “Traffic volume and traffic speed in Tokyo.”